

Relationship between pulse-wave velocity and arterial elasticity

F. J. Callaghan L. A. Geddes C. F. Babbs J. D. Bourland

Biomedical Engineering Center, Purdue University, West Lafayette, IN 47907, USA

Abstract—Pulse wave velocity (PWV) was measured *in situ* in 11 isolated canine common carotid arteries. Seven arteries exhibited a linear PWV/pressure function at pressures ranging from 0 to 200 mm Hg. Four arteries yielded a linear relationship between PWV and pressure between 1 and 100 mm Hg; for these vessels the relationship was nonlinear at higher pressures. Seven arteries (five from the group which was linear up to 200 mm Hg and two from the group which was linear up to 100 mm Hg) were excised and pressure/volume measurements were made *in vivo*. Using pressure/volume data, the Moens-Korteweg equation was evaluated as a predictor of the PWV/pressure relationship over the linear region. An expression was developed to enable prediction of the pressure/volume relationship using the coefficients at the linear PWV/pressure function; these predictions were evaluated. We found that, for this range, the Moens-Korteweg equation provides a very good basis for predicting the increase in PWV with increasing bias pressure. In addition, we found that the pressure/volume relationship of common carotid arteries is well represented by an exponential of the form $V/V_0 = Ke^{zt(P)}$, which was derived as the inverse solution to the Moens-Korteweg equation.

Keywords—Arterial elasticity, Pulse-wave velocity

Med. & Biol. Eng. & Comput. 1986, 24, 248–254

1 Introduction

THE MEASUREMENT of blood pressure has long provided information of significant clinical value. To date, however, there is no technique for monitoring blood pressure over long periods of time which is suitable for both invasive and noninvasive applications. Problems with chronic direct measurement techniques include seal leakage, thromboembolisation and lack of a suitable pressure reference when implantation is desired. Chronic noninvasive indirect measurements require periodic cuff inflation and deflation and cannot provide pressure measurements on a beat-by-beat basis.

Pulse-wave velocity, the speed at which a pressure pulse propagates along an elastic artery, depends on the prevailing (diastolic) pressure within the artery. Blood pressure can be monitored continuously with extravascular pulse pickups and time-domain techniques for determining pulse-wave velocity (GEDDES *et al.*, 1981). Accordingly, the objectives of this study were threefold:

- to establish *in situ*, under controlled conditions, an accurate functional description of the relationship between pulse-wave velocity (PWV) and pressure
- to evaluate the PWV predictions of the Moens-Korteweg equation, given measured pressure/volume relationships
- to evaluate the inverse solution of the Moens-Korteweg equation, given a measured functional relationship between PWV and pressure.

It is well known that the velocity of a pulse wave in the arterial system depends on blood pressure. In 1878 MOENS and KORTEWEG independently derived an equation which describes the relationship between the elastic modulus of a thin-walled, distensible, fluid-filled tube and the velocity of a pressure pulse induced within it. The equation is

$$c = \sqrt{\left(\frac{tE}{2\rho r}\right)} \quad (1)$$

where c = pulse wave velocity, t = wall thickness, r = lumen radius, ρ = density of the fluid within the lumen and E = Young's modulus. The assumptions which underlie the Moens-Korteweg equation, and their applicability to common carotid arteries, are addressed in the Discussion section.

POSEY and GEDDES (1973) developed an expression for the elastic modulus of a thin-walled tube in terms of its dimensions and pressure/volume relationships:

$$E = \frac{2}{t} \frac{dP}{dV} \sqrt{\left(\frac{V^3}{\pi L}\right)} \quad (2)$$

where V = tube volume, L = tube length, r = wall thickness and P = pressure. Substituting this expression into the Moens-Korteweg equation, one obtains an equation which describes pulse-wave velocity in terms of the volume V and compliance dV/dP of the arterial segment:

$$c = \sqrt{\left(\frac{1}{\rho} \frac{dP}{dV} V\right)} \quad (3)$$

When pressure P is expressed in mm Hg, density ρ in

First received 11th November 1983 and in final form 16th April 1985

© IFMBE: 1986

g cm⁻³ and velocity c in m s⁻¹, this expression becomes

$$c = 0.3652 \sqrt{\left(\frac{1}{\rho} \frac{dP}{dV} V\right)} \quad (4)$$

In this paper, eqn. 4 will be used to predict the velocity/pressure relationship of an artery from pressure/volume data collected *in vitro*; these predictions will be compared with velocities measured *in situ*.

It has been shown by GEDDES *et al.* (1981) that, for physiological pressures in the dog aorta, PWV is linearly related to pressure; therefore a specific relationship must exist between the pressure and volume of an arterial segment. Squaring eqn. 3 we obtain

$$c^2 = \frac{1}{\rho} \frac{dP}{dV} V \quad (4a)$$

Since velocity is a linear function of pressure, we have

$$c = mP + b \quad (5)$$

where m and b are the slope and intercept, respectively, of the velocity/pressure relationship. Thus

$$(mP + b)^2 = \frac{1}{\rho} \frac{dP}{dV} V \quad (6)$$

Separating variables and integrating, one obtains

$$\ln V = -\frac{1}{\rho m(mP + b)} + \frac{k}{\rho} \quad (6a)$$

where k is a constant of integration. The boundary conditions are

$$V = V_0 \quad \text{when} \quad P = 0$$

Thus

$$\ln V_0 = -\frac{1}{\rho m b} + \frac{k}{\rho}$$

and subtraction of this equation from the previous one yields

$$\frac{V}{V_0} = e^{1/\rho m [1/(b - 1/mP + b)]} \quad (7)$$

Eqn. 7 will be used to predict the pressure/volume relationship when the slope m and intercept b of the velocity/pressure function are known; these predictions will be compared with the pressure/volume relationship measured *in vitro*.

2 Materials and methods

2.1 In situ velocity/pressure measurements

Six mongrel dogs were anaesthetised with sodium pentobarbital (30 mg kg⁻¹ IV). The neck was incised bilaterally to expose the cephalad and caudal aspects of the two common carotid arteries. Femoral artery pressure was continuously monitored with a pressure transducer (P23ID, Gould Instruments, Oxnard, California), while midaxillary safety-pin electrodes provided ECG signals.

Following surgery, the animals were heparinised (1 mg kg⁻¹) and the two ends of a single common carotid artery were exposed and ligated; a stiff-walled catheter was introduced into each end of the isolated arterial segment. Separation between catheter tips was made as large as possible by placing the cephalad catheter close to the carotid sinus. The caudal placement was typically under the first rib. Once placed, the catheters and artery were

repositioned in the incision to keep the arterial segment straight and to maintain normal tissue contact against the vessel. Special care was taken while placing the catheters and ligatures to avoid occluding other smaller vessels traversing the carotid sheath, helping to ensure perfusion through the carotid vasa vasorum. These precautions were taken to obtain an *in situ*, isolated arterial segment with a reasonable level of perfusion and innervation. Catheter diameters were selected which were as close as possible to carotid lumen diameters. 1 cm of overlap between the catheter tip and arterial segment was provided; ligatures were placed at the point of maximum overlap so that the catheter opening would be within an arterial segment with viscoelastic properties uninfluenced by the isolation apparatus.

The apparatus for establishing bias pressure in the isolated arterial segment and measuring pulse-wave velocity is illustrated in Fig. 1. All tubing, including the arterial segment, was filled with heparinised (10 mg l⁻¹), lactated Ringer's solution (sodium lactate 77.5 mg ml⁻¹, NaCl 150 mg ml⁻¹, KCl 7.5 mg ml⁻¹, CaCl₂ 5 mg ml⁻¹; density \approx 1.00 gm cm⁻³). The system was arranged so that it could be flushed and pressurised as desired.

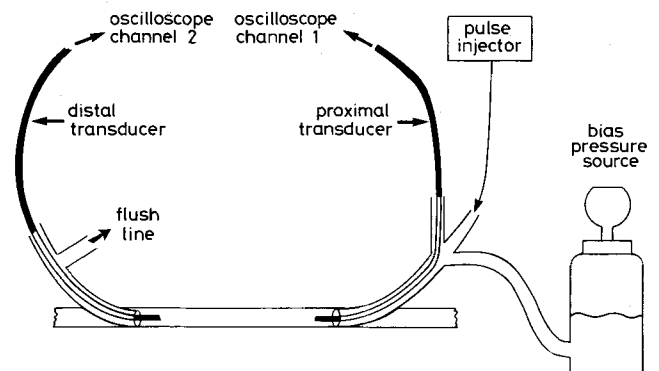


Fig. 1 Simplified representation of the *in situ* preparation. Bias pressure may be manually applied by compression of the rubber bulb. The proximal transducer is at the cephalad aspect of the common carotid artery. A signal from the pulse injector is used to trigger the oscilloscope.

A catheter-tip pressure transducer (Millar MIKRO-TIP model PC-350, Millar Instruments, Houston, Texas) was introduced into each end of the isolated arterial segment so that the sensing element was 1 cm into the vessel at the cephalad end (proximal to the pulse source) and was immediately inside the vessel at the caudal end (distal to the pulse source). These two sensing locations were chosen to preclude displacement of the pulse peak which may arise from reflections. The position of the proximal catheter tip is not critical; the delay time between the incident pulse and the arrival of the first reflected wave was several times greater than the pulse width (\approx 25 ms). Consequently, displacement of the pulse peak (due to superposition of incident and reflected waves) was not a problem at the proximal sensing location. At the distal location, the spacing between the catheter-tip sensor and the stiff-walled catheter introducer is more critical, since the introducer acts as a reflector. The impedance of this distal termination was designed to be large and real by obtaining small dimensional tolerances between the catheter transducer and the catheter introducer. Thus, when the transducer tip is slightly inside the vessel, superposition of incident and reflected pulses yields amplitude distortion but peak location (in time) is unchanged. This technique allows maximal transducer separation (for increased temporal resolution)

while errors in pulse peak identification (due to superposition of incident and reflected waves) are minimised.

Pressure pulses were introduced into the isolated arterial segment by an electronically controlled, solenoid-driven syringe. The amplitude and duration of these pulses could be precisely controlled. Pressure-pulse signals were displayed on a storage oscilloscope (Tektronix model 5115, Portland, Oregon). The height of a fluid reservoir was adjusted to establish a zero bias pressure inside the vessel; once established, positive bias pressures were obtained by pressurising this reservoir with a compressible rubber bulb. At a given bias pressure, five pulse-wave velocity measurements were made. The pulse (amplitude < 20 mm Hg) was generated by suddenly injecting a small volume of fluid into the arterial segment. By measuring the time delay between the appearance of a pulse at the two transducers transit time, the delay between the peaks of the pulses, was determined. Since the distance between transducers was known (typically 10 cm), velocity was readily calculated. Bias pressure was raised in 20 mm Hg increments from 0 to 200 mm Hg and pulse-wave velocity was measured at each bias pressure.

After collecting data for one carotid artery, measurements were made on the contralateral artery. Then the arteries were measured for their *in situ* length, excised, and stored in cold lactated Ringer's solution (<2 days) until pressure/volume measurements were made. Four vessels were damaged during excision, rendering them unsuitable for *in vitro* measurements

2.2 In vitro pressure/volume measurements

Fig. 2 illustrates the apparatus used for determining pressure/volume relationships. Carotid arteries used in the pulse-wave velocity studies were tethered (in air, 25°C) to a mounting device, taking care to stretch the vessel to its original *in situ* length. A catheter-tip pressure transducer (Millar Mikro-Tip model PC-350, Millar Instruments, Houston, Texas), introduced into one end of the vessel,

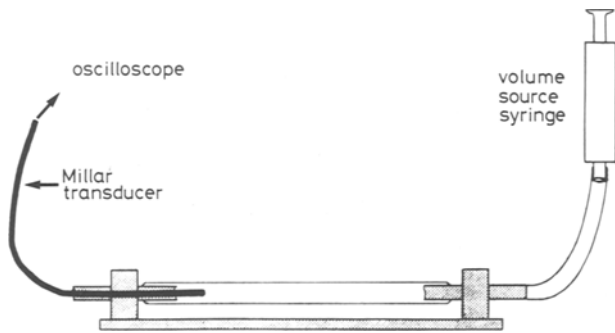


Fig. 2 Apparatus for determining *in vitro* pressure/volume relationships

was used to display pressure on a storage oscilloscope (Tektronix model 5115). The other vessel opening was connected to a syringe which served to introduce measured volumes of lactated Ringer's solution (density 1.00 g cm⁻³).

Determination of V_0 , the zero-pressure volume of the arterial segment, was accomplished by filling the segment with fluid until the pressure just began to exceed zero. Fluid was then withdrawn into a syringe until evacuation caused the vessel to collapse along its entire length. The fluid added to the syringe was taken as V_0 . Once V_0 was established, a steady zero-pressure bias was readily maintained and data collection consisted of injecting known volumes into the vessel and measuring the rise in pressure on the oscilloscope. The duration of a given volume injection was short (<100 ms) to minimise any decay in pressure which may result from stress relaxation and fluid leakage through the vasa vasorum. In this study, a volume injection was repeated four times; volumes were increased incrementally until pressures near 200 mm Hg were reached.

3 Results

3.1 In situ velocity/pressure measurements and comparisons with predictions from *in vitro* pressure/volume measurements

Pulse-wave velocity against bias pressure, measured *in situ* on 11 arteries, is listed in Table 1. Least-squares linear regression coefficients are found in Table 2. Correlation coefficients greater than 0.90 were obtained for seven of the arteries; representative data for a typical vessel are shown in Fig. 3. Note that the velocity/pressure relationship is essentially linear over the range of physiological pressures. Four vessels exhibited nonlinearity in the velocity/pressure relationship as shown in Fig. 4. For these vessels, linearity is evident up to pressures near typical diastolic; above this, the velocity/pressure relationship appears to follow a higher-order function.

Table 2 Linear equations for velocity/pressure curves

Artery	Slope, $\text{ms}^{-1} \text{mm Hg}^{-1}$	Intercept ms^{-1}	Correlation coefficient
1 left	0.1331	-1.5954	0.8732
1 right	0.0678	2.3559	0.9825
2 left	0.0978	0.8864	0.8911
3 left	0.1867	-4.3233	0.8336
3 right	0.2343	-8.3359	0.8998
4 left	0.0831	0.2182	0.9411
4 right	0.0875	0.1934	0.9500
5 left	0.0576	1.9065	0.9784
5 right	0.0463	2.4281	0.9882
6 left	0.0552	2.4264	0.9964
6 right	0.0684	1.5081	0.9877

Table 1 Pulse-wave velocity (m s^{-1}) as a function of bias pressure. Each velocity represents a mean of five trials

Artery	Pressure, mm Hg											
	0	5	20	40	60	80	100	120	140	160	180	200
1 left	1.55	—	2.77	3.80	4.84	5.78	8.12	12.05	19.42	21.83	30.83	—
1 right	2.61	—	4.67	5.39	6.20	7.25	8.13	9.57	11.70	13.13	15.08	16.83
2 left	3.54	—	4.79	5.53	6.11	6.68	8.05	9.21	12.50	16.00	19.27	25.64
3 left	1.53	—	3.50	4.31	5.36	6.89	8.97	11.75	14.89	23.75	34.08	42.75
3 right	—	—	3.30	4.59	6.03	7.25	9.80	14.25	16.86	25.65	37.84	48.73
4 left	—	2.55	3.19	3.89	5.09	5.74	6.81	7.54	9.76	12.59	16.81	20.26
4 right	—	2.75	3.30	3.98	4.98	5.80	6.98	8.41	10.72	13.98	16.80	21.07
5 left	—	2.84	3.49	4.37	5.28	6.13	6.98	8.03	9.48	10.67	12.67	14.68
5 right	—	3.02	3.69	4.24	5.24	5.95	6.74	7.37	8.55	9.59	11.07	12.46
6 left	1.92	2.44	3.54	4.70	5.91	7.22	7.98	8.93	9.88	11.21	12.50	13.40
6 right	—	2.19	3.35	4.42	5.60	6.90	7.90	8.83	10.28	12.02	14.30	16.34

Predictions of the velocity/pressure relationship from pressure/volume data were calculated using eqn. 4. For a given point on the pressure/volume curve, dP/dV was evaluated as the slope of the line between adjacent points.

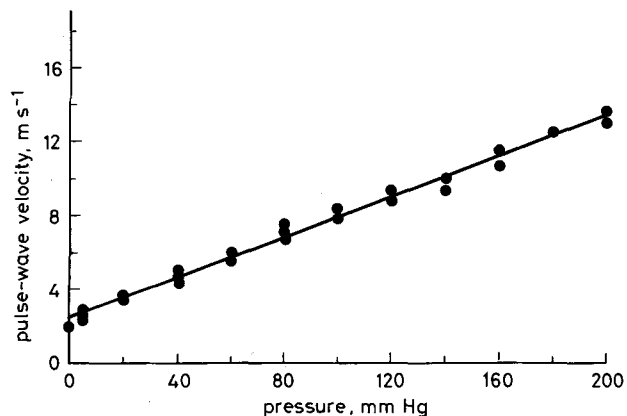


Fig. 3 Velocity/pressure relationship which was linear over the entire range of physiological pressures. This vessel is representative of seven out of 11 arteries. The data are for five trials

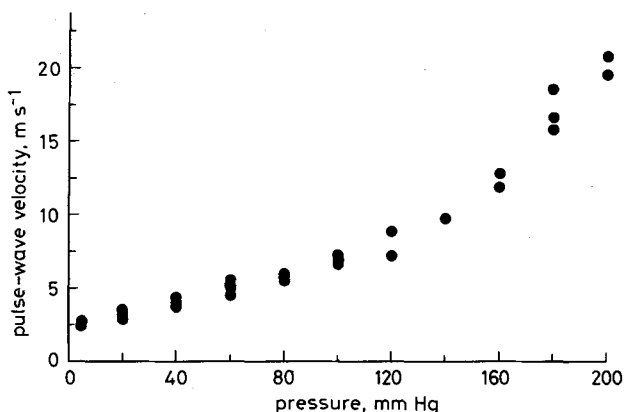


Fig. 4 Velocity/pressure relationship for an artery which was linear up to pressures near diastolic. This vessel is representative of four out of 11 arteries

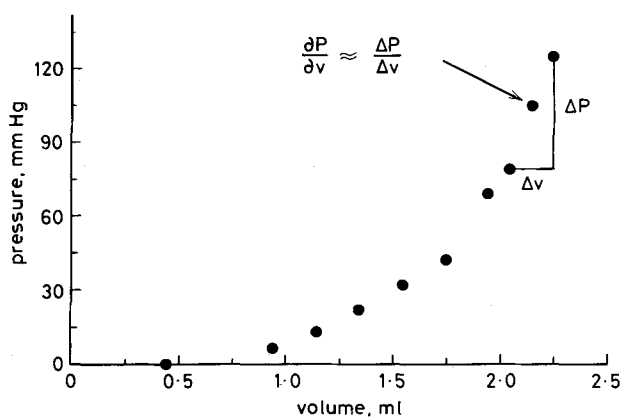


Fig. 5 Pressure/volume curve for a typical artery. Estimations of dP/dV are used to predict velocity/pressure relationships

Table 3 Comparison of slopes from in situ velocity/pressure experiments with estimated slopes from in vitro pressure/volume data

Artery	Measured slope, $\text{ms}^{-1} \text{mm Hg}^{-1}$	Estimated slope $\text{ms}^{-1} \text{mm Hg}^{-1}$
3 right	0.067*	0.057
4 left	0.050**	0.057
4 right	0.087	0.081
5 left	0.058	0.059
5 right	0.046	0.037
6 left	0.055	0.068
6 right	0.068	0.077
mean	0.0616	0.0623
Standard error	0.0052	0.0056
Standard deviation	0.0138	0.0148

* pressure < 100 mm Hg
** pressure < 140 mm Hg

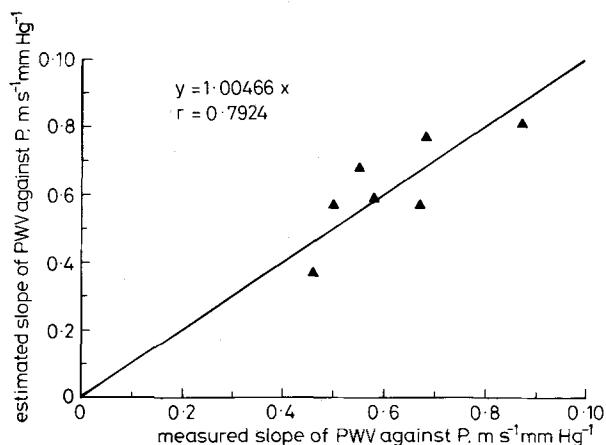


Fig. 6 Proportional linear regression analysis used to evaluate the predictions of the Moens-Korteweg equation. A slope of 1.0 is expected when the predictions are exact

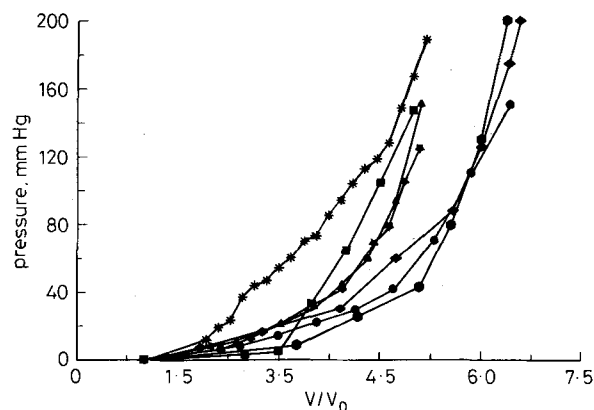


Fig. 7 Measured pressure/volume relationships for seven arteries. V_0 is the zero-pressure volume of the arterial segment

expected when the predictions are exact. For these data, $a = 1.0047$ and r (correlation coefficient) = 0.7925.

It is evident that the Moens-Korteweg equation, when expressed in terms of pressure and volume (eqn. 3), provides a good prediction of pulse-wave velocity as a function of pressure.

3.2 In vitro pressure/volume measurements and comparisons with predictions from in situ velocity/pressure measurements

Pressure/volume data, measured *in vitro* on seven arteries, are shown in Fig. 7. Volumes are expressed as V/V_0 to normalise the data for undistended volume differ-

Fig. 5 depicts a dP/dV estimation for a typical artery. Table 3 compares measured slopes with predicted slopes. A two-tailed, paired-difference *t*-test indicates that these paired data are not significantly different ($\alpha = 0.05$).

To evaluate the ability of the Moens-Korteweg equation to predict PWV, a proportional linear regression analysis was performed. A linear regression line (of the form $y = ax$) was calculated for 'predicted slope' as a function of 'measured slope' (Fig. 6). A regression slope of 1.0 is

ences among the arterial segments. In addition, the inverse Moens-Korteweg solution (as derived in eqn. 5) does not permit the determination of V_0 ; it is necessary to express measured volumes as V/V_0 to compare the measured P/V relationship with the predicted one.

Predictions of pressure/volume relationships from the velocity/pressure function are obtained from eqn. 5. Application of the Moens-Korteweg equation requires that the artery behave as a perfectly elastic tube at all pressures; definition of V_0 as the zero-pressure volume may be inappropriate if the artery has not yet begun to be stretched. To determine the volume at which stretching begins dP/dV was plotted as a function of V (Fig. 8). dP/dV remains essentially constant over small volumes. At larger volumes dP/dV becomes a higher-order function. The volume at which stretching begins was estimated as the point at which dP/dV begins to exhibit a positive slope. On average, this volume, occurring at a pressure of 9.2 mm Hg, was 2.9 times the undistended volume.

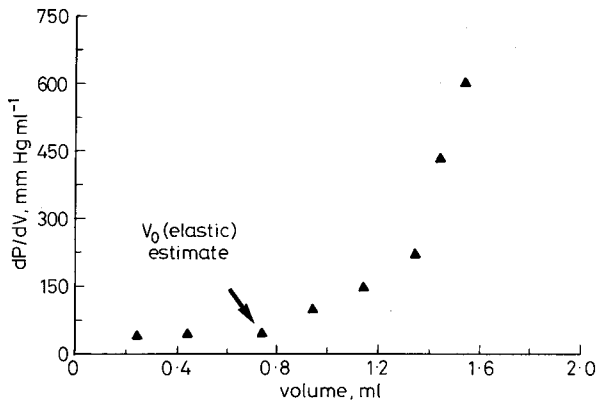


Fig. 8 dP/dV as a function of V for one artery. Estimates of the volume at which arterial stretching begins are obtained from these curves

Fig. 9 compares the predicted and measured pressure/volume functions when V_0 is interpreted as the volume at which stretching begins. Each function appears to be an exponential and plots of $\ln(P)$ against V/V_0 , illustrated in Fig. 10, yield the least-squares linear regression slopes found in Table 4. Correlation coefficients greater than 0.96

Table 4 Slope of $\ln(P)$ against V/V_0 for measured and predicted cases. V_0 is interpreted as the volume at which stretching begins. Correlation coefficients greater than 0.96 were obtained in each case

Artery	Measured slope	Estimated slope
3 right	3.330	3.099
4 left	1.741	1.802
4 right	1.803	2.066
5 left	2.055	2.293
5 right	1.362	2.081
6 left	2.036	2.877
6 right	3.198	2.321
Mean	2.218	2.263
Standard error	0.2841	0.1756
Standard deviation	0.7516	0.4646

were obtained in all cases. Comparisons between the measured and predicted relationships were based on the exponential character of these functions.

To evaluate the pressure/volume predictions, a paired-difference t -test and a proportional linear regression line (Fig. 11) were determined for the data of Table 4. The paired difference t -test indicates that these paired data are not significantly ($=0.05$) different. A regression slope of

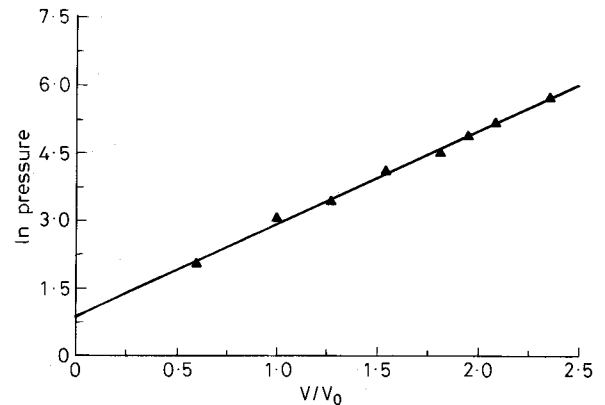


Fig. 10 A typical $\ln(P)$ against V/V_0 relationship which is linear over the range of physiological pressures, indicating an exponential relationship between pressure and volume

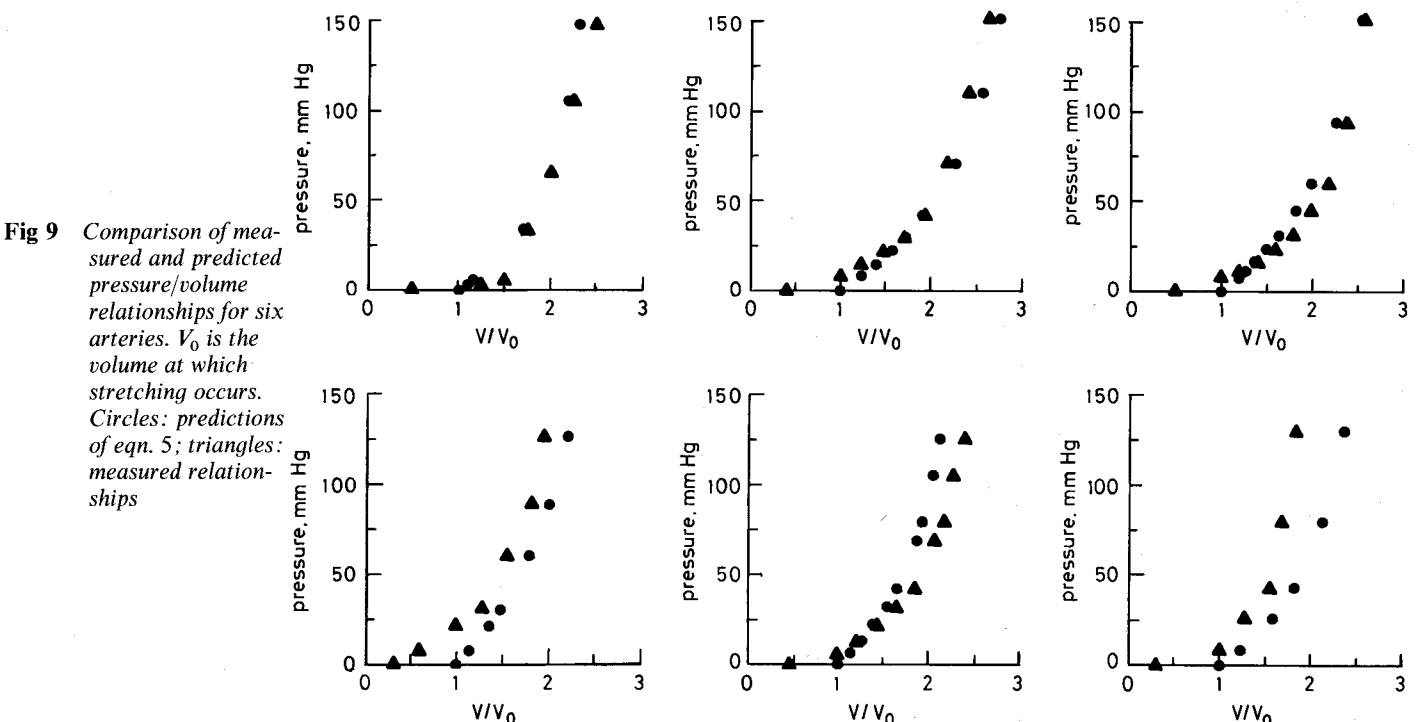


Fig. 9 Comparison of measured and predicted pressure/volume relationships for six arteries. V_0 is the volume at which stretching occurs. Circles: predictions of eqn. 5; triangles: measured relationships

1.0049 (correlation coefficient = 0.6336) indicates that reasonably accurate predictions of pressure/volume relationships can be obtained when the coefficients of a linear velocity/pressure function are known.

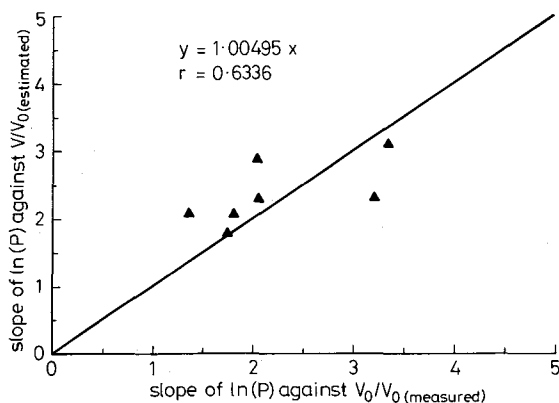


Fig. 11 Proportional linear regression analysis used to evaluate predictions of pressure/volume relationships when the slope and intercept of the velocity/pressure function are known. A slope of 1.0 is expected when the predictions are exact

4 Discussion

Many studies have investigated pulse-wave velocity *in situ* using natural cardiac pressure pulses; a review of these was presented by GEDDES *et al.* (1981). However, small errors are inherently introduced which are related to the presence of bulk blood flow. Flow velocities of the order of 0.25 ms^{-1} are commonly found in large elastic arteries and must be subtracted from the measured values to obtain true pulse-wave velocity. Simultaneous changes in cardiac output and peripheral resistance may alter bulk flow velocity while pressure remains constant. Although these flow-related variations are small (typically <10 per cent), they are not necessarily insignificant, especially at low diastolic pressures. Because it was desired to evaluate the Moens-Korteweg equation as a predictor of PWV, such errors were unacceptable for this study. In addition, we sought to evaluate the inverse solution of the Moens-Korteweg equation, given a functional relationship between pressure and PWV; this inverse solution requires an accurate measured relationship between PWV and pressure.

The Moens-Korteweg equation predicts the relationship between PWV, modulus of elasticity and dimensions of an elastic tube. This equation is based on energy conservation principles and, as derived, requires three critical assumptions about the elastic tube:

- the fluid within the tube is incompressible
- the wall thickness is small with respect to the lumen radius
- the tube is perfectly elastic.

At physiological pressures, incompressibility of the blood is a good assumption for all pressures within the arterial tree. The validity of assumptions 2 and 3, when applied to an arterial segment, depend largely on the region of the vascular bed from which an arterial segment is selected. The assumption of a small wall-thickness/lumen-radius ratio allows one to neglect the energy-consuming effects of radial wall acceleration. A small ratio implies that the inertial resistance of the vessel wall and the force required to accelerate the wall mass is negligible. In addition, an artery will behave more like a rigid pipe than an elastic tube as this ratio becomes large. It is well known that the large

calibre 'elastic' arteries near the heart exhibit a much smaller wall-thickness/lumen-radius ratio than the smaller peripheral 'muscular' arteries (ATTINGER, 1968).

Assumption (c) is most applicable for the large central arteries but it is important to note that no artery is perfectly elastic. To be perfectly elastic, the stress/strain function must not exhibit hysteresis. Arteries do exhibit a slight stress/strain hysteresis; the area of the hysteresis loop represents the energy lost in overcoming the viscosity of the elastic elements. However, the central 'elastic' arteries exhibit much less hysteresis than peripheral 'muscular' arteries BADER, 1963. As the amount of arterial smooth muscle increases, assumptions of 'perfect elasticity' become less valid.

Common carotid arteries were selected for this study because they qualify reasonably for the assumptions just described. In addition, these vessels are readily accessible, do not have large branches where reflections could arise and are virtually uniform in diameter and wall thickness for long segments. Peripheral muscular arteries, because of larger wall-thickness/lumen-radius ratios and higher smooth muscle content, do not satisfy the Moens-Korteweg assumptions very well. In addition, it is expected that alterations in sympathetic tone may change their viscoelastic properties.

The *in situ* studies described in this paper have demonstrated that, under controlled conditions, the velocity/pressure function is essentially linear up to and slightly beyond typical diastolic pressure. In only four of the 11 arteries, pulse-wave velocity increased nonlinearly at supradiastolic pressures. This behaviour is expected in an elastic tube as it approaches its elastic limit at high pressures. For these vessels, estimates of PWV (obtained from pressure/volume data) were calculated only over the linear region. We have found that in this region the Moens-Korteweg equation provides a good theoretical model.

Based on the coefficients of a linear PWV/pressure function, the inverse solution of the Moens-Korteweg equation was evaluated. In the derivation of eqn. 5 it was necessary to assume that the vessel begins to stretch (i.e. behave as an elastic tube) as the pressure begins to exceed zero. This is, in fact, not the case; stretching appears to begin at some small non-zero pressure (typically <10 mm Hg). As a first approximation, one can obtain good estimates of pressure/volume relationships from the linear coefficients of the PWV/pressure function.

In conclusion, we have found that the Moens-Korteweg equation provides a good basis for prediction of the increase in pulse-wave velocity with increasing bias pressure. In addition, we have found that the pressure/volume relationship of common carotid arteries is well represented by an exponential of the form $V/V_0 = Ke^{af(P)}$.

Acknowledgments—This study was supported by grant HL29275-01 from the National Heart, Lung & Blood Institute, Bethesda, Maryland, USA, who also supported Dr. C. F. Babbs under Research Career Development Award HL00587.

References

- ATTINGER, E. O. (1968) Analysis of pulsatile blood flow. In *Advances in biomedical engineering and medical physics, Vol. 1*. Wiley-Interscience, New York, 1–59.
- BADER, H. (1963) The anatomy and physiology of the vascular wall. In *Handbook of physiology, Section 2, vol. II*. American Physiological Society, Washington DC, 865–890.
- GEDDES, L. A., VOELZ, M. H., BABBS, C. F., BOURLAND, J. D. and TACKER, W. A. (1981) Pulse transit time as an indicator of arterial blood pressure. *Psychophysiology*, **18**, 71–74.

KORTEWEG, D. J. (1878) *Über die Fortpflanzungsgeschwindigkeit des Schalles in elastischen Röhren. Ann. Phys. Chem.* **5**, 525–542.

MOENS, A. I. (1878) *Die Pulscurve.* E. J. Brill, Leiden, 87–95.

POSEY, J. A. and GEDDES, L. A. (1973) Measurement of the modulus of elasticity of the arterial wall. *Cardiovasc. Res. Ctr. Bull.*, **11**, 83–103

Authors' biographies



Frank Callaghan received the MS degree in Biological Science in 1978 and the MSEE degree in Electrical Engineering in 1982, both from Purdue University. He is currently a Senior Research Engineer with Cordis Corporation, Miami, Florida USA. His interests include biomedical measurement and instrumentation, cardiac pacing and electrophysiology.



Dr. Leslie A. Geddes is the Showalter Distinguished Professor of Bioengineering and Director of the Biomedical engineering Center at Purdue University. Born in Scotland and educated in Canada, Dr. Geddes holds the Bachelor's and Master's degrees in Electrical Engineering from McGill University and the Ph.D. degree in Physiology from Baylor University College of Medicine, Houston, Texas.



Dr. Charles F. Babbs was born in Toledo, Ohio on the 6th July 1946 and holds the M.D. and M.S. (Anatomy) degrees from Baylor College of Medicine, the Ph.D. in Pharmacology from Purdue University, and the B.S. in Experimental Psychology from Yale University. He is an Associate Research Fellow in the Purdue Biomedical Engineering Center, an instructor in medicine at Indiana University School of Medicine and a licensed physician in Texas and Indiana. His research is in the areas of cardiopulmonary resuscitation, tumour blood flow, ventricular defibrillation and implanted therapeutic devices. His current projects are an automatic implanted blood pressure controller and an automatic implanted defibrillator.



Dr. Joe Bourland is co-ordinator for engineering at the Biomedical Engineering Center at Purdue University. He received a B.A. in Science/Engineering from Rice University and the Ph.D. in Physiology from Baylor College of Medicine in Houston, Texas. His research interests are ventricular fibrillation/defibrillation, electrosurgery, automatic control of blood pressure and cardiac output. He is author of more than 50 publications in these areas and holds several patents.